ELSEVIER

Bioelectrochemistry and Bioenergetics 46 (1998) 91–103

BIOELECTROCHEMISTRY AND BIOENERGETICS

The influence of electrode polarisation on dielectric spectra, with special reference to capacitive biomass measurements
I. Quantifying the effects on electrode polarisation of factors likely to occur during fermentations

Christopher L. Davey *, Douglas B. Kell

Institute of Biological Sciences, University of Wales, Aberystwyth, Ceredigion, Wales, SY23 3DA, UK

Received 30 May 1998; accepted 9 June 1998

Abstract

Electrode polarisation can interfere significantly with the measurement of the dielectric properties of biological systems, and in particular with the dielectric estimation of microbial biomass. We show that electrode polarisation can be modelled by a power law and that the parameters of this model can be simply modified to give reliable and intuitive measures of the magnitude ($^{L}C_{p}$) and rate of fall of polarisation with increasing frequency (^{h}f). Importantly and surprisingly, although the *magnitude* of electrode polarisation depends strongly on the conductance of the medium and the material of the electrodes, above a certain value of medium conductance (of some 3–7 mS, conductivity = 3.7–8.7 mS cm^{-1}), the value of ^{h}f is a constant and independent of the conductance of the medium. It is also independent of the electrode metal in the probes, which probe was used, the ionic and other components in the medium, the electrode interface current density, the cell constant, the presence of fouling materials and whether or not any electrolytic cleaning pulses had been applied. This permits one simply to correct for the electrode polarisation present in dielectric spectra and which may sometimes be seen during dielectric biomass measurements.

Keywords: Dielectric spectroscopy; Electrode polarisation; Biomass estimation

1. Introduction

The on-line and real-time measurement of the biomass content of fermentations is still an active area of research [1–10]. New sensors are continuously being developed and the already established technologies are constantly being improved. The reason for this need for innovation is that the fermentation industry works with a very broad range of cell types using a wide range of culturing conditions and under an ever-growing blanket of regulatory requirements.

To fit easily into an already established fermentation installation, a biomass monitoring system must be generic and capable of working via the currently available probe ports, must not pose a significant contamination risk, be capable of withstanding in-situ the high temperatures and pressures or caustic nature of sterilisation processes, and the probe materials must be inert. The equipment must be supplied in a form that can easily be incorporated into (and survive in) a fermentation hall environment. This is true before any consideration can be given to its ability to work with the cell system being monitored.

The fermentation broth itself is a particularly hostile environment for any sensor to work in. The growth of the cells and the feeding and control regimes used ensure that it is an ever-changing environment. The presence of vigorous and fluctuating aeration and time-dependent temperature profiles is a particular problem. The medium used can be highly viscous and often contains a wide range of non-biomass solids and immiscible liquids, particularly at the start of the fermentation. The medium's constitution can change markedly as the cells grow and consume its components.

An ideal measuring system should be capable of working with a wide variety of cell types ranging from bacterial cells and yeasts, through filamentous fungi and bacteria to animal and plant cells, in both free and immobilised forms. The ability to measure a wide range of biomass concentra-

* Corresponding author

0302-4598/98/$19.00

tions is important as is the inclusion of an in-situ cleaning system that can remove cellular growth on the sensing probe.

A widening body of literature has demonstrated that the measurement of biomass by use of a capacitive probe provides the best and most generic method in practical situations. Sensor methods based on two-pin electrodes and electromagnetic coupling are being developed but as yet have not been refined enough to work in anything other than laboratory model systems. The most highly developed technology that has found practical utility in industry is the Biomass Monitor (BM). This instrument fulfils the majority of the criteria outlined above and published work has shown it to work well for bacteria [11], yeast [12–16], filamentous fungi and bacteria [17,18], animal [19,20] and plant cells [21,22], immobilised cells [23,24], for solid substrate fermentations of filamentous fungi [25–27], and in assessing cytotoxicity [28–31]. Its major applications in industry so far [32] have been for controlling the pitching of yeast slurries in brewing [16,33] and for monitoring microbial fermentations in the pharmaceutical industry [17].

Details of biological dielectrics [34–39] and the theory behind capacitive (dielectric) biomass measurements can be found in Refs. [3,4,6,11,12,21,22,38,40–46]. For the purposes of this paper, a simplified heuristic model will be described. Cells in a suspension can be regarded as having a three-component structure. Outside and inside the cells is a conducting aqueous ionic medium, the former being the suspension medium, the latter the cell cytoplasm. Surrounding the conducting cell core is the thin essentially non-conducting plasma membrane. This means that a cell suspension can be regarded from an electrical point of view as a suspension of spherical capacitors containing a conducting matrix surrounded by a conducting suspension medium. To make measurements on this system, one typically applies an electric field via a set of electrodes. The resulting electrical current paths have two routes through the suspension, either around the cells via the external conductance or through them via the membrane capacitance and internal and external conductances. At low radio frequencies and below (< 0.1 MHz), the cell membrane has a very low admittance, most of the current flows around the cells and as the membrane capacitance is nearly fully charged, the capacitance of the suspension is very high. The more cells that are present per unit volume, the more spherical capacitors are charged and so the higher is the capacitance of the suspension. Thus, the low-frequency capacitance gives a measure of cellular volume fraction. As non-biomass material (including necromass) lacks an intact plasma membrane, it does not give a significant capacitance contribution. At frequencies above 10 MHz, the membrane capacitance is shorted out, the induced charge held by the membranes is very low and so the capacitance of the suspension approaches that of the water in the suspending medium.

From these arguments, one expects the capacitance of a cell suspension to go from a high low-frequency plateau to a low high-frequency one. This fall in capacitance as a function of increasing frequency due to the shorting of the membrane capacitance is called the β-dispersion (Fig. 1). The high-frequency residual capacitance due mainly to water dipoles is called C_∞. The height of the low-frequency plateau above C_∞ is called the capacitance increment ΔC_β and its magnitude is proportional to the biomass content of the suspension. The frequency when the fall from $\Delta C_\beta + C_\infty$ to C_∞ is half-completed is called the critical frequency f_c The steepness with which capacitance falls as frequency increases is described by the Cole–Cole α value. This has values in the range $0 =< \alpha < 1$ and is supposed to reflect the distribution of relaxation times in the suspension due to heterogeneity (but see Refs. [36,38,47–49]). Shown on Fig. 1 are the curves for α equals 0 (no distribution of relaxation times) and α equals 0.2. Increasing α from 0 does not change ΔC_β, f_c or C_∞; its major effect on the α equals 0.2 plot, shown on the figure, is that in the frequency window shown, the low-frequency plateau is not achieved.

From these arguments, one can see that to estimate the biomass concentration in a fermentation broth, all one has to do is measure the ΔC_β of the suspension. On the BM, this is done in either of two ways. Fig. 2a shows a β-dispersion with a spot-measuring frequency (typically 0.4 MHz) marked by an arrow and the capacitance at that frequency marked by a dot on the curve. As one can see, the capacitance at the measuring frequency is a good approximation of the ΔC_β and hence, biomass concentra-

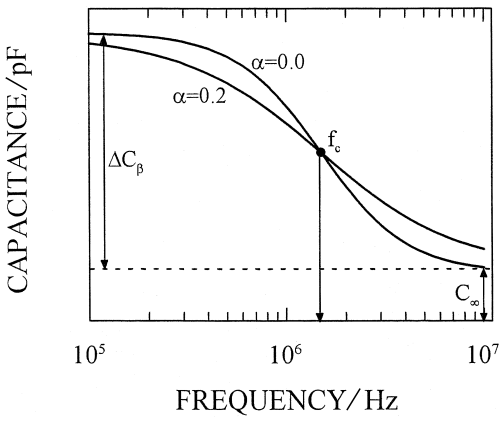

Fig. 1. The β-dispersion of biological cells. The two curves shown both have the same high-frequency plateau (C_∞) and low-frequency plateau height above this (ΔC_β), and both reach the mid-point of their capacitance fall at the same frequency (f_c). What differs between them is the magnitude of their Cole–Cole α values which give a measure of how rapidly the capacitance falls as frequency increases. The α values shown are 0 (a Debye-type dispersion) and 0.2 which fall within the range typical for biological cell suspensions of 0 to 0.3. The higher the α value, the less steep is the fall and the less likely is it that the high- and low-frequency plateaus are going to be reached within a restricted frequency interval like that shown on the figure, or available on a BM.

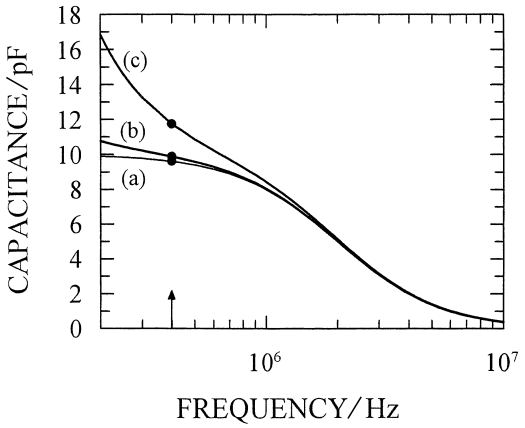

Fig. 2. (a) A β-dispersion which is uncorrupted by electrode polarisation. At the biomass-measuring frequency (indicated by the vertical arrow), the capacitance provides a good estimate of ΔC_β and hence, of biomass concentration. (b) Most fermentations have some electrode polarisation present which causes the capacitance to tip up as frequency decreases. The biomass-measuring frequency is picked to give a good estimate of biomass while minimising the contribution from the electrodes at that frequency. (c) Serious electrode polarisation has swamped the β-dispersion and made biomass estimation at the spot frequency unreliable.

tion. In reality, what one does for these single-frequency biomass measurements, and what has been done on this figure, is to back off the capacitance due to the suspending medium to zero at the spot-measuring frequency prior to inoculation. Then any changes in the capacitance at that frequency reflects changes in ΔC_β and hence, biomass concentration. The second capacitive biomass method uses two frequencies, the spot-measuring frequency as before and also a high-frequency reference (10 MHz). From Fig. 2, it will be seen that the difference in the capacitance between the spot-measuring frequency (0.4 MHz) and that at 10 MHz also gives a good estimate of ΔC_β.

For both methods to work reliably, the spot biomass measuring (low) frequency should be well into the low-frequency plateau of the β-dispersion, since the f_c of the dispersion can move with changes in the medium conductance. If the measuring frequency was on the falling part of the dispersion, then movements in the f_c could cause significant changes in the capacitance measured at the spot frequency and result in corresponding errors in the biomass determination.

To be well onto the plateau means that for most β-dispersions, one must use a measuring frequency below 0.5 MHz. This, however, forces one to use a frequency region in which the polarisation of the measuring electrodes can contribute a significant capacitance that can interfere with the biomass measurements [3,4,44]. This electrode polarisation effect results largely from the charged electrodes attracting around themselves a counter-layer of ions which acts electrically as a capacitor/resistor network in series with the biological suspension one is trying to measure. Reviews of the electrode polarisation mechanism in the context of biological dielectric measurements can be found in Refs. [3,35,40,41,50–54].

For a given electrode material, the most important factor that controls the magnitude of this electrode polarisation is the conductance of the suspending medium [50]: the higher the conductance, the larger the polarisation, until it completely swamps the β-dispersion. Fig. 2b shows the β-dispersion curve in (a) but with the small amount of polarisation typical of most fermentations. At the spot-measuring frequency, the polarisation's contribution to the signal is quite low and does not result in a significant error in biomass estimation. The real problems occur when the medium conductance is very large and the biomass concentration is comparatively low. This is illustrated Fig. 2c where the β-dispersion line (a) has been swamped by polarisation. Under these conditions, the polarisation results in a large error in the estimated biomass concentration using the spot-measuring frequency. Since the magnitude of this polarisation can be time-dependent as the medium conductance changes or as the electrodes become fouled, it is clear that dielectric biomass estimation can be rendered much more difficult.

This pair of papers aims at addressing this problem in two stages. In the first paper, we develop a means of describing and quantifying the electrode polarisation in a simple compact manner which would be intuitive to a user and simple to do routinely. This methodology is then used to study the effects that the conditions pertaining to fermentations have on electrode polarisation. The second paper [55] then uses these findings to design mathematical models of electrode polarisation that can be implemented to remove or to reduce the electrode polarisation automatically.

2. Methods

2.1. Chemicals and yeasts used

All the salts used were of analytical grade and all solutions and suspensions were made up in distilled water. The salt solutions used, other than KCl, were adjusted to the same 1 MHz conductance as 120 mM KCl (with the BM in high cell constant mode) with the relevant solid salt.

A totally lysed yeast suspension was made using a variety of lytic stresses, as previous experiments had shown that this was the only way to ensure complete cell lysis and hence, no β-dispersion. The suspension was made as follows. Allinsons dried active baking yeast was obtained locally and made up in distilled water to give a suspension dry weight of 101 mg ml^{-1}. This was then boiled for 70 min over a Bunsen burner, cooled and frozen. The next day, the suspension was thawed and diluted with distilled

water to give an equivalent dry weight of 35 mg ml^{-1}. The suspension was then autoclaved for 30 min at 15 lb/in^2 before being cooled and refrozen. On the day of use, the yeast was thawed, allowed to reach room temperature and diluted 1 in 3 in 120 mM KCl before its conductance was adjusted to that of 120 mM KCl (at 1 MHz, with the BM in high cell constant mode) using solid KCl or distilled water.

2.2. Electrodes and their preparation

The same three-standard BM electrodes (produced by Aber Instruments, Science Park, Aberystwyth, Ceredigion, SY23 3AH, UK) were used throughout the experiments. These probes has a 25-mm diameter cylindrical epoxy shaft with four cylindrical metal electrode pins projecting from the end. Two probes had solid pure gold pins while the other had pins of solid pure platinum. One gold probe had been used extensively and had developed a thin layer of amorphous gold on its pin surfaces, giving them a matt finish. This probe was thus called the mAu probe. The second gold pin probe was brand new and had electrode pins with smooth shiny surfaces and so was called the sAu probe. The platinum probe was also new and had smooth shiny pins; it was called the sPt probe.

Electrode polarisation is very sensitive to electrode fouling [56] and so before each experiment, the probes were cleaned very thoroughly using the following procedure which we found to be reliable. (1) Rinse probe and pins with running cold tap water followed by rubbing the pins down with washing-up liquid (using a paper towel) and then rinsing as before. (2) Next, the probe is treated with Concentrated Persil Colour (with stain release system) clothes washing liquid (Lever Brothers). This contains soap and polycarboxylates ($< 5\%$), non-ionic surfactant (5 to 15%), anionic surfactant and zeolite (15 to 30%), protease, lipase, amylase and cellulase. An amount of 0.6 ml of the Persil is added to 100 ml of tepid tap water and the probe is suspended in it for 5 min. The pins are then rubbed down with a paper towel and the diluted Persil before reimmersing for further 5 min. (3) Rinse thoroughly in running cold tap water followed by a rinse in distilled water. The pins are then inspected to ensure that they are free from any adhering material.

Before and during the experiments, the probes were never allowed to dry out. If storage was required during an experiment, the probes were suspended in distilled water. Before such storage and between transfers to different treatments during the experiments, the electrodes were washed in distilled water. At the end of each experiment, the probes were washed in distilled water and stored dry under cover to keep dust off the pins.

2.3. Electrical measurements

All electrical measurements were made with the same BM 214A dielectric spectrometer (Aber Instruments, Science Park, Aberystwyth, Ceredigion, SY23 3AH, UK). All capacitance and conductance values are for admittance domain measurements. Unless otherwise stated, the BM was configured with low-pass noise filtration off, single frequency/scanning mode active, display and output set to absolute capacitance ('C mode'), the high cell constant mode set and the electrolytic cleaning system deactivated. For all experiments, the BM had been set-up and left on for several hours prior to use to allow it to warm up properly.

For all the experiments in this paper, the BM was set to high cell constant mode and run under computer control using a program called BMScan. This was written in-house in the Microsoft QuickBasic 4.5 compiler and allowed the BM to be controlled, and data retrieved, via a DT2811 PGH A/D, D/A converter card (Data Translation, The Mulberry Business Park, Wokingham, Berkshire, RG41 2GY, UK) in a 486 IBM compatible PC. The program was configured to scan the BM through the same 50 frequencies for each experimental run. These frequencies were picked by the program so that they were evenly spaced on a log frequency scale between 0.2 and 10 MHz. The order in which the 50 frequencies were scanned was randomised by the program so that each scan used a different *ordering*. During a scan, the program waited 4.5 s after switching frequencies for the BM to settle before taking and averaging 10 replicate readings at 0.1 s apart.

The cell constants of the three probes were estimated using 10 mM KCl solutions of known temperature (i.e., known conductivity) at 1 MHz as described in Refs. [3,41]. With the BM set to high cell constant mode, all the probes had a cell constant of 1.24 cm^{-1}; in low mode, the mAu probe's cell constant was 0.71 cm^{-1}.

The electrolytic cleaning system of the BM was never used during the preparation of the electrodes nor during the experiments unless otherwise stated. In experiments where they were used, the pulses were manually applied 10 times in succession, with the full cleaning cycle completed before the next pulse was activated. After the final pulse, any gas bubbles adhering to the probes were shaken off and the capacitance and conductance signals at 0.2 MHz allowed to stabilise before the probes were scanned.

The experiments were carried out in a 600-ml glass beaker containing 500 ml of the relevant solution or suspension. The BM probe was situated so that its tip was central in the volume of liquid, so that the electric field it produced did not couple into the glass or flea used. The liquid was stirred at a constant 300 rpm and periodic checks were made to ensure that the electrode pins were free from air bubbles. The BM head amplifier earth was clipped to the metal top of the stirrer [3].

2.4. Initial analysis of the capacitance spectra

To extract the electrode polarisation data from the frequency scans, the data had to be compensated for the

distortions present in the capacitive spectra. The methods used to do this are illustrated in Fig. 3a which shows a frequency scan for 56 mM KCl measured in high cell constant mode under computer control. The electrode polarisation data are confined to the frequency range below about 1 MHz. The epoxy material making up the probe shaft itself disperses in the frequency range of interest and distorts the polarisation curve. Previous experiments have shown that this dispersion is essentially linear in the frequency range of the BM. One can therefore compensate for it by fitting a straight line to the capacitance data in the frequency range above the polarisation but below frequencies at which inductances distort the data at higher frequencies. The data used to get this linear fit are shown between the arrows on Fig. 3a and the fit to these data is the straight line shown. By subtracting this line from the frequency scan, one not only removes the probe dispersion but also subtracts the offset under the polarisation curve due to the probe construction and the water in the solution used. Fig. 3b shows the data in Fig. 3a after this has been done and these types of *probe-compensated data* are the basis of all subsequent analyses in this paper.

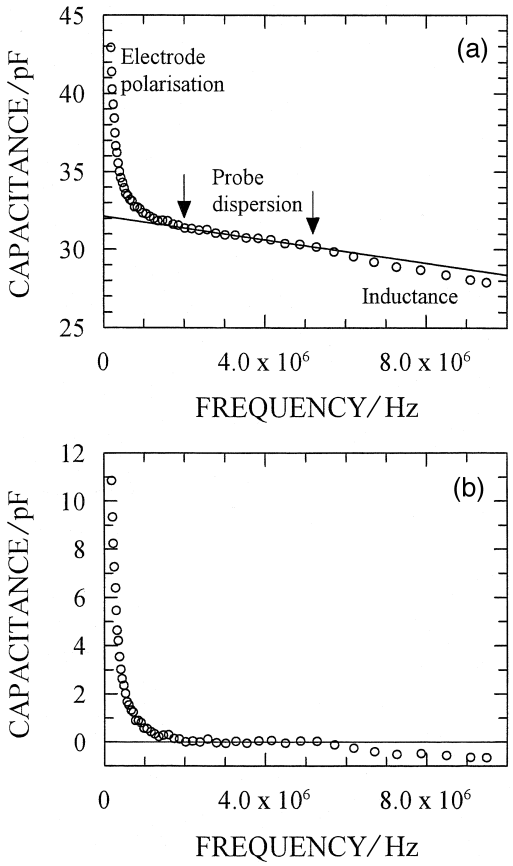

Fig. 3. (a) A frequency scan of a 56 mM KCl solution using the mAu probe. At frequencies below about 1 MHz, the capacitance is dominated by electrode polarisation. At frequencies above 6 MHz, the BM's baseline tips down due to inductances. In the frequency range between these two ranges (marked by arrows), the BM baseline is seen to slope slightly due to the dispersion of the plastic material, making-up the shaft of the electrode probe. This dispersion has been shown to give a straight line over the BM's frequency range. The data between the arrows were fitted by linear regression ($r = -0.99$) to give the line shown on the figure. This line was then subtracted from the raw scan data to give the probe compensated data shown on (b).

3. Results and discussion

3.1. Effect of medium conductance on electrode polarisation

The aim of the work described in this paper was to create models that could be used to quantify electrode polarisation and then use these as a means to develop techniques that could be used to remove the contribution of electrode polarisation to the capacitance spectra of biological cell suspensions. This would allow better biomass estimation and the generation of better-quality dielectric spectra.

The first step in such an approach would be to fit the electrode polarisation to a mathematical function (such as a power or exponential function) that describes the frequency dependence of the polarisation in terms of parameters that quantify the magnitude of the polarisation and how fast it falls with increasing frequency. The more these parameters could be made intuitive to BM users, the more useful they would be. Thus, the first step required is to find a suitable mathematical function that describes the electrode polarisation over a wide range of polarisation magnitudes. The easiest way to generate the required data is to change the conductance of the medium being used.

Computer-controlled frequency scans were done using the mAu probe on aqueous KCl solutions that covered the entire conductance range of the BM (in high cell constant mode). Nineteen evenly spaced KCl concentrations were used starting at 10 mM and ending with 175 mM. To ensure that the experiment showed up any day-to-day variations in the response of the electrodes, the experiment was split into three parts. The second part was 4 days after the first and the third part a further 2 days later. In between days, the probe was stored dry as described in Section 2.

Table 1 shows in detail how the KCl concentrations were distributed across the three parts of the experiment and the random order the solutions were used in on each day. The random ordering was used to highlight and eliminate any memory effects that the electrode surfaces may have for previously used solutions. This complemented the random order of the frequencies in each scan as described in Section 2. The 175-mM KCl concentration was likely to give the largest polarisation and so be most sensitive to day-to-day variations in the electrodes and was thus used as an inter- and intra-experiment part control. The fact that it was considered that chemometric or artificial neural network models of the polarisation might be necessary [57,58] dictated that the whole KCl range was

Table 1
The KCl solutions used in the three parts of the experiment along with the order in which they were used

mM KCl	Part (1) order	Part (2) order	Part (3) order
10	1st	–	–
19	–	2nd	–
28	–	–	7th
38	2nd	–	–
47	–	3rd	–
56	–	–	2nd
65	6th	–	–
74	–	1st	–
83	–	–	5th
93	5th	–	–
102	–	7th	–
111	–	–	4th
120	4th	–	–
129	–	4th	–
138	–	–	3rd
148	3rd	–	–
157	–	6th	–
166	–	–	8th
175	7th	5th	1st and 6th

covered on each day. Not only would such models include the day-to-day variation but parts (1) and (2) could be used to produce a model which could be checked by predicting the part (3) data, etc. [9].

Fig. 3a and b show the results for 56 mM KCl. All the spectra from the experiment were converted to their probe-compensated form as shown in Fig. 3b, using the procedure described in Section 2. To model the resulting polarisation curves, one must separate the polarisation data below 1 MHz from the residual inductances that are present above 6 MHz (see Fig. 3b). At the same time, one must characterise the polarisation curves in a succinct and unambiguous form.

The shape of the capacitance curve below 1 MHz on Fig. 3b suggests that the power law model found to be applicable to other electrode systems by other workers [59,60] (see also the earlier work on electrode impedance reviewed in Refs. [51,53]) would be of use here. The power law has the form:

$$^{f}C_{p} = {}^{1\,Hz}C_{p}\, f^{p} \qquad (1)$$

where $^{1\,Hz}C_{p}$ is the capacitance due to polarisation at 1 Hz, f is the applied frequency (in Hz), p is the power term (dimensionless) and $^{f}C_{p}$ is the frequency-dependent polarisation capacitance (in pF). As p is dimensionless, what we call $^{1\,Hz}C_{p}$ in fact has units of pF Hz^{-p} and so is numerically equal to the polarisation capacitance at 1 Hz. $^{1\,Hz}C_{p}$ is used as a designation as it emphasises the fact that functionally, Eq. (1) acts as a constant capacitance (the capacitance at 1 Hz) scaled by the variable f^{p} term. Linearised, Eq. (1) becomes:

$$\log\left(^{f}C_{p}\right) = \log\left(^{1\,Hz}C_{p}\right) + p\log(f) \qquad (2)$$

Eq. (2) was used to test the model on the *probe-compensated data* like those shown on Fig. 3b. To do this, the data at frequencies above where the capacitance first becomes zero or negative were discarded. Fig. 4 shows the data on Fig. 3b plotted in the form of Eq. (2). The data between the arrows were used to produce the straight line fit shown. As can be seen, a very good straight line is achieved at frequencies below about 1 MHz where the electrode polarisation dominates the capacitance spectrum. Thus, the power law model provides an excellent way of characterising polarisation curves and indeed, this is in line with previous studies [51,59]. The line's y-axis intercept is $\log(^{1\,Hz}C_{p})$, which gives a measure of the magnitude of the polarisation in $^{1\,Hz}C_{p}$. The line's slope is the power p which gives a measure of how rapidly the polarisation capacitance falls as frequency increases. Using these best fit $^{1\,Hz}C_{p}$ and p values in Eq. (1) allows the polarisation data to be plotted as a function of frequency. This is done for the fit on Fig. 4 in Fig. 5 where the data points (open circles) shown are the *probe-compensated data* from Fig. 3b. Once again, the power law provides a very good fit to the data.

Fitting the *probe-compensated data* to an exponential model, in a similar way as was used for the power law model, failed to give a good fit to the data, indicating that electrode polarisation does not follow an exponential law.

All the frequency scans from this experiment were analysed using the power law model to give p and $^{1\,Hz}C_{p}$ values. In all cases, the power law provided an excellent fit to the data. Fig. 6 is a plot of the fitted p values vs. the conductance of the KCl solutions at 1 MHz for the three parts of the experiment. A full discussion of this plot will be provided later in the context of the half frequency (^{h}f) which is derived directly from it but is far more intuitive to

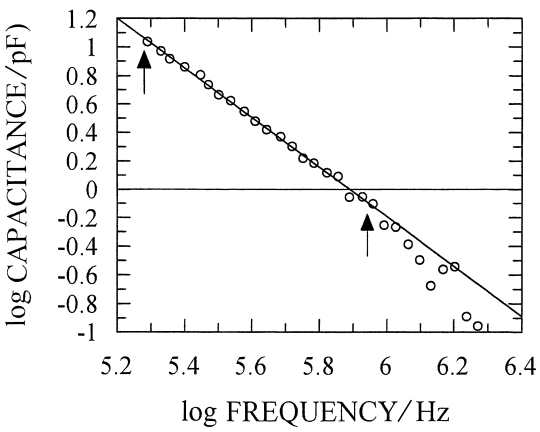

Fig. 4. The positive valued *probe-compensated data* from Fig. 3b replotted on a log/log plot to show how the electrode polarisation seen below 1 MHz gives a straight line, indicating a power law model applies. The data between the arrows were fitted by linear regression ($r = -1.00$) to give the straight line shown. The slope of the line gives p and the y-intercept, $\log(^{1\,Hz}C_{p})$.

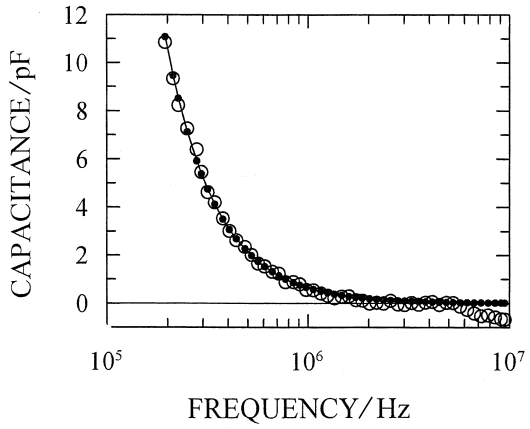

Fig. 5. The *probe-compensated data* from Fig. 3b (open circles) shown with the best fit power law model of the electrode polarisation (dots and lines). This was derived using the p and ${}^{1\,\mathrm{Hz}}C_\mathrm{p}$ values from the linear fit on Fig. 4 which were then put into Eq. (1) and plotted as a function of frequency. A log frequency axis is used to emphasise the frequency range where electrode polarisation dominates the data.

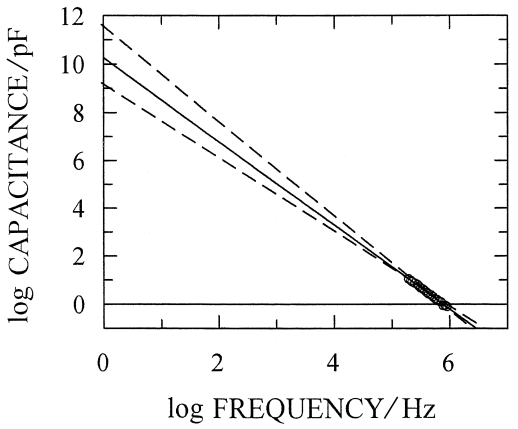

Fig. 7. This is Fig. 4 replotted but showing only the data (open circles) used to give the straight line fit shown on that figure (solid line). The x-axis has been extended to show the extrapolation of the fitted straight line back to the y-axis to give $\log({}^{1\,\mathrm{Hz}}C_\mathrm{p})$. The two dotted lines show how plausible fits to the data could, when extrapolated over such a large frequency range, give very different estimates of the magnitude of the polarisation (as measured by ${}^{1\,\mathrm{Hz}}C_\mathrm{p}$). Note that a log y-axis is used and so even minor differences in the y-intercept values could give very large differences in the estimated ${}^{1\,\mathrm{Hz}}C_\mathrm{p}$ values derived from them.

use. It will suffice to note that above about 7 mS, the p value is a constant of about -2 (mean $= -1.99$, SD $=$ 0.060), which puts Eq. (1) into the form of an inverse square law: ${}^{\mathrm{f}}C_\mathrm{p} = {}^{1\,\mathrm{Hz}}C_\mathrm{p}(1/f^2)$.

There is a problem with using ${}^{1\,\mathrm{Hz}}C_\mathrm{p}$ as a measure of the magnitude of the electrode polarisation. In Fig. 4, there is a little noise on the data which means that another scan of the same solution might produce a slightly different fitted line. Within the BM's frequency window (see Fig. 4), the lines would not be significantly different, but when extrapolated back to 1 Hz, as required to get ${}^{1\,\mathrm{Hz}}C_\mathrm{p}$; these differences could become quite large. This would produce large artefactual differences in the magnitude of polarisation where in fact, in the range where data were taken, there were no significant differences. Just how large these extrapolations are is illustrated by Fig. 7 which shows the linear fit on Fig. 4 extrapolated back to 1 Hz, along with the data values used for the fitting (between the arrows on Fig. 4).

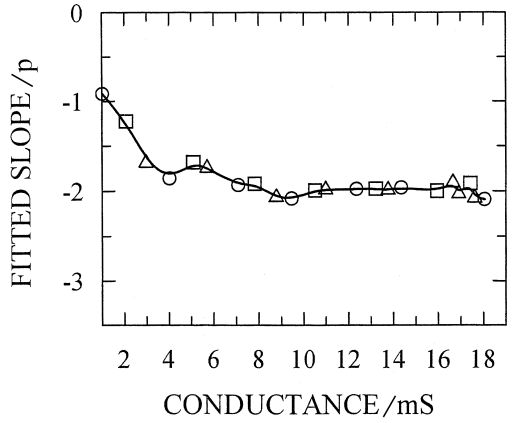

Fig. 6. The p values for the KCl solutions shown on Table 1; derived using the procedures shown on Figs. 3–5, plotted against the conductance of the solutions as measured at 1 MHz. The circles are for part (1) of the experiment, the squares are part (2) and the triangles part (3). The interpolated line is a four-spline to all the data.

To make the characterisation of the electrode polarisation curves using the power law model more reliable, one needs a measure of the magnitude of the polarisation that characterises it in the frequency range where we actually have data. At the same time, a more intuitive form of p, the measure of how steep is the fall in capacitance with increasing frequency, would be useful. Ideally, this should enable one to look at an actual set of BM polarisation data (such as Fig. 3a or b) and see straight away how the measure relates to them. This would not only make searching for trends in the data far easier but it would also enable BM users to monitor the polarisation they are getting with their electrodes quickly and routinely.

The logical measure of the magnitude of the polarisation in the BM's frequency range is to quote it as the extent of the polarisation at the lowest frequency used. The lowest frequency is called ${}^{\mathrm{L}}f$ (in Hz) and the polarisation capacitance at it, ${}^{\mathrm{L}}C_\mathrm{p}$ (in pF). As a power law is being used to model the polarisation, one does not have a 'half-life' to characterise the rate of fall of capacitance with increasing frequency but by analogy, one could use the frequency when the capacitance at ${}^{\mathrm{L}}f$ (i.e., ${}^{\mathrm{L}}C_\mathrm{p}$) has halved; this is called the half-frequency (${}^{\mathrm{h}}f$). Fig. 8 is an illustration of how ${}^{\mathrm{L}}f$, ${}^{\mathrm{L}}C_\mathrm{p}$ and ${}^{\mathrm{h}}f$ relate to a set of *probe-compensated data* in the BM's frequency range.

For very rough and ready routine monitoring of electrode polarisation, one would use a high conductance solution where the polarisation swamps any baseline slope. One could then estimate ${}^{\mathrm{L}}C_\mathrm{p}$ as the difference in capaci-

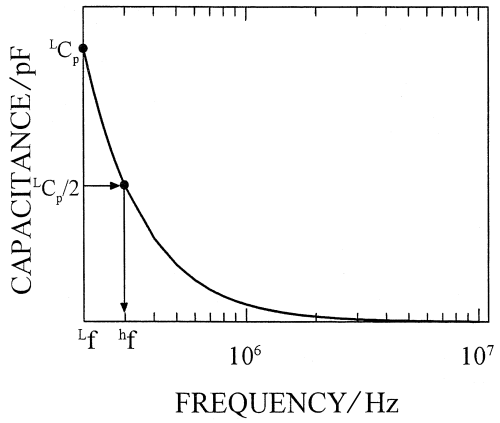

Fig. 8. One solution to the extrapolation problem shown on Fig. 7 is to use estimates of the magnitude of the polarisation and how fast it changes with frequency that apply to the frequency range where one actually has data. The curve shown illustrates how *electrode polarisation* changes as a function of frequency in the BM's frequency range (0.2 to 10 MHz). The lowest frequency where one has data (^{L}f) is used to estimate the magnitude of the polarisation as measured by the polarisation capacitance ($^{L}C_p$) at that frequency. A more intuitive measure of how fast the polarisation capacitance changes as a function of frequency than p is the half-frequency (^{h}f). This is the frequency when the capacitance at ^{L}f (i.e., $^{L}C_p$) has halved. The variable ^{h}f is not a half-life and only has meaning (as does $^{L}C_p$) when quoted in conjunction with its equivalent ^{L}f value.

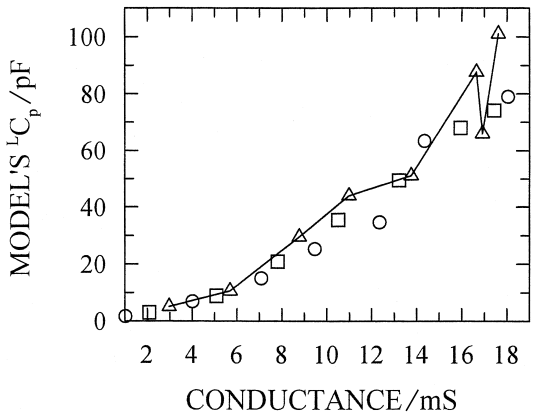

Fig. 9. The $^{L}C_p$ values for the KCl solutions shown on Table 1, derived as described in the text using an ^{L}f of 0.20 MHz. The values are plotted against their conductance values at 1 MHz with circles being part (1), the squares part (2) and the triangles and line part (3). As expected, the magnitude of the polarisation increases as the conductance increases but as the line through the part (3) data demonstrates, there is a lot of variation.

tance between an ^{L}f of 0.2 MHz and the end of significant polarisation at about 2 MHz. One would then estimate ^{h}f by setting the BM to 2 MHz and dialling the frequency back towards 0.2 MHz until the capacitance had risen by half this difference.

For detailed studies of polarisation, one needs to relate $^{L}C_p$ and ^{h}f to the fit of the power law model to real BM data as illustrated on Fig. 4. To do this, one needs to convert the $^{1\,Hz}C_p$ and p values that such a fit gives directly to $^{L}C_p$ and ^{h}f. To get $^{L}C_p$ (in pF), one selects the lowest frequency (^{L}f, in Hz); which for the BM is typically 2.10^5 Hz, and inserts it along with the best fit $^{1\,Hz}C_p$ (in pF) and p values, into Eq. (1) and then calculates $^{L}C_p$ directly. The derivation of how one gets ^{h}f from p is a little more complicated and is detailed in Appendix A. The result of the derivation there is that p and ^{h}f (in Hz) are related by Eq. (3):

$$^{h}f = {}^{L}f\,2^{\frac{-1}{p}} \qquad (3)$$

The p and $^{1\,Hz}C_p$ values for all the KCl solutions were converted to their equivalent ^{h}f and $^{L}C_p$ values using the BM's lowest frequency of 2.10^5 Hz as ^{L}f. Fig. 9 is a plot of the $^{L}C_p$ values vs. the 1 MHz conductance of the KCl solutions, over the three parts of the experiment. As expected, there is a general increase in the magnitude of the polarisation as the solution conductance increases. There is, however, significant day-to-day variation and some large changes even within one part of the experiment.

Fig. 10 is a plot of the ^{h}f values vs. the 1 MHz conductance of the KCl solutions, over the three parts of the experiment. Importantly, there is virtually no inter- or intra-experimental variation in these values. Above about 3–7 mS, the ^{h}f is almost constant at about 0.28 MHz (relative to the ^{L}f of 0.2 MHz). This is quite remarkable given the wide variations in the magnitude of the polarisation over this conductance range. Also, the BM's electronics are configured to increase the current density across the electrode interfaces as the conductance increases which will itself alter the polarisation. The tip-up in ^{h}f at lower conductances is not due to polarisation but reflects a baseline anomaly of the BM itself which becomes evident

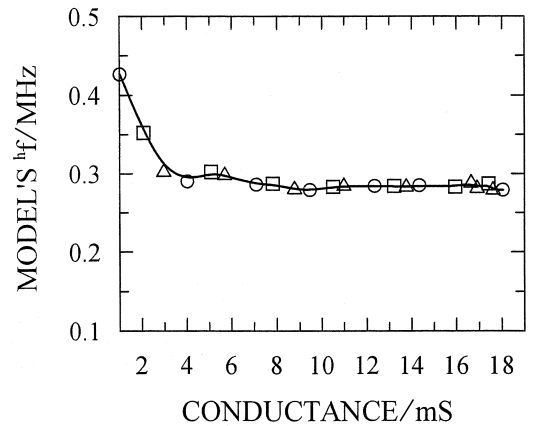

Fig. 10. The ^{h}f values for the KCl solutions shown on Table 1, derived as described in the text using an ^{L}f of 0.2 MHz. The values are plotted against their conductance values at 1 MHz with circles being part (1), the squares part (2) and the triangles part (3). The line through the data is a five-spline. Above about 7 mS (and possibly down to 3 mS), the ^{h}f is constant, the tip up at low conductances is due to a baseline effect on the BM.

only at low conductances. From Fig. 9, one can see that these elevated ${}^{h}f$ values correspond to small 'polarisation' magnitudes.

3.2. Effects on polarisation of factors that might be encountered in fermentations

The ${}^{h}f$ and ${}^{L}C_{p}$ method of characterising electrode polarisation was then used to quantify the effects on the polarisation resulting when the electrodes are exposed to the environmental changes that are likely to occur during fermentations. In addition, one must access the effect of changing the probe, as may occur in real fermentation environments from time to time.

To investigate these possible influences, an experiment was carried out under computer control as described in Section 2. The BM's electrolytic cleaning pulses were applied during this experiment. These pulses generate electrolysis bubbles at the pin's surfaces which dislodge any adhering fouling material, but also are known (and are designed) to alter the magnitude of the electrode polarisation. Thus, the order in which each part of this experiment was done in is very important and this dictates the order of the descriptions of these experiments below. In all cases,

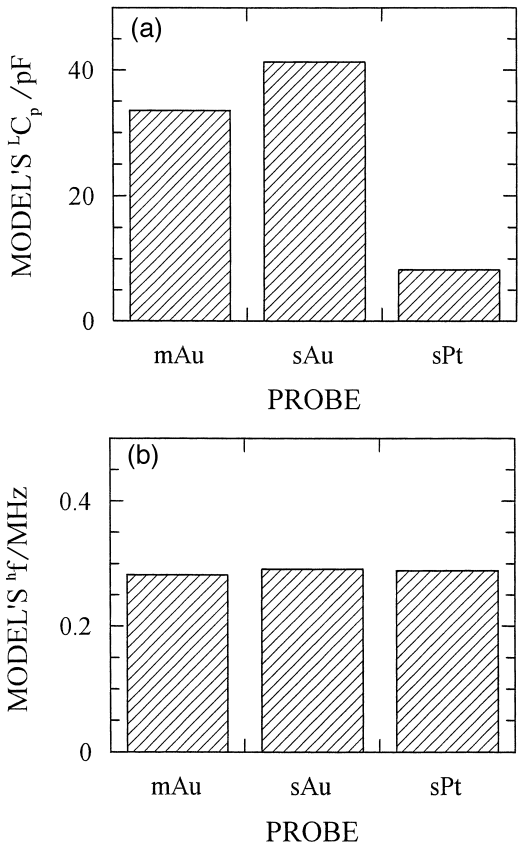

Fig. 11. The effect of changes in the probe and the metals used on the ${}^{L}C_{p}$ (a) and ${}^{h}f$ (b) as judged using a 120-mM KCl solution. The probes were used in the order shown from left to right.

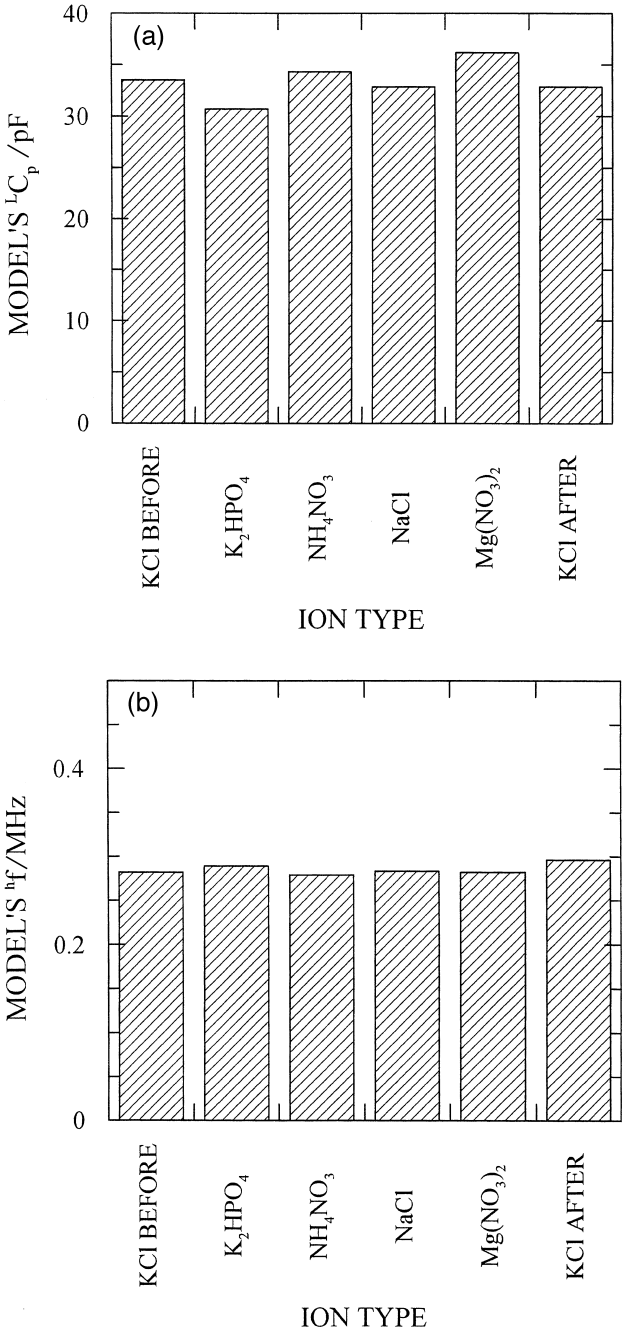

Fig. 12. The effect of changes in the ions in solution on the ${}^{L}C_{p}$ (a) and ${}^{h}f$ (b) of the mAu probe. All the solutions had the same conductance as 120 mM KCl at 1 MHz. The solutions were used in the order shown from left to right.

the capacitance spectra fitted the power law model very well and the data were analysed to give ${}^{h}f$ and ${}^{L}C_{p}$ values relative to a ${}^{L}f$ value of 2.10^{5} Hz as described previously.

Firstly, the effect of changing probes (and probe material) was investigated by scanning the mAu, sAu and sPt probes in 120 mM KCl. The order in which the probes were used was randomised. The results are shown in Fig. 11a and b. From Fig. 11a, it can be seen that there is quite a large variation in the magnitude of the polarisation even

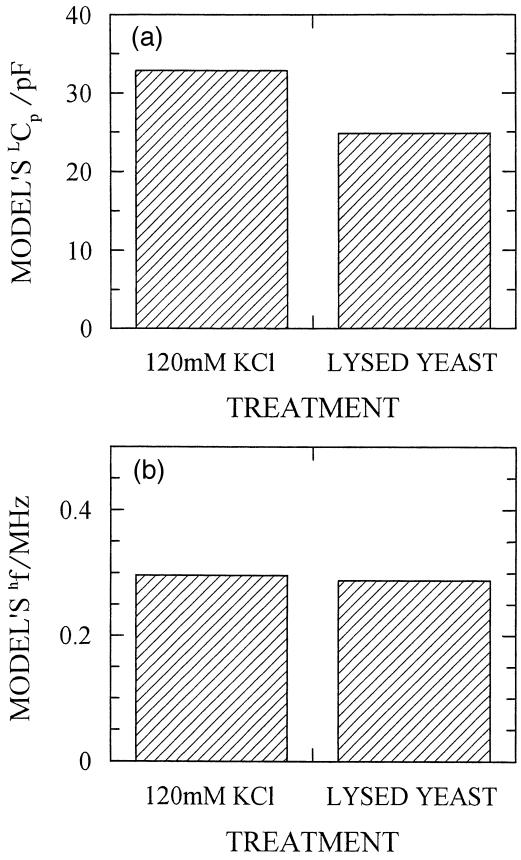

Fig. 13. The effect of exposure to electrode fouling materials on the $^{L}C_{p}$ (a) and ^{h}f (b) of the mAu probe. The lysed yeast had the same conductance as 120 mM KCl at 1 MHz. The solutions were used in the order shown from left to right.

between gold probes. Whether the matt or smooth finish has any significant effect here cannot be ascertained from just the two probes used. Certainly, roughing the surface of probe pins is a standard way of reducing their polarisability and indeed forms the rationale for blacking platinum pin electrodes [41]. The large reduction in polarisation magnitude on using platinum pins was expected, since this metal is known not to polarise as greatly as other metals. However, the sPt probe, while giving very significant improvement over gold, still had sufficient polarisation to pose possible problems when measuring small biomass concentrations. However, Fig. 11b gives the ^{h}f values for the three probes, where it can be seen that although the polarisation $^{L}C_{p}$ values are very different, these ^{h}f values are all identical with the values in the KCl concentration experiment (which was in fact performed about 1 1/2 months previously).

Next, the mAu probe was exposed to solutions containing ions of different sizes as this would be expected to effect the polarisation by altering the Stern layer at the pin's surfaces. As controls, 120 mM KCl was scanned at the start and end of the experiment. The ionic solutions were adjusted using the relevant solid salt to have the same 1 MHz conductance as the KCl solution, as described in Section 2. This means that the same current densities should be crossing the pin/aqueous interface in all cases. The order the salt solutions were scanned was randomised. Fig. 12a shows that the $^{L}C_{p}$ values were again different for the various solutions, although none of these differences were particularly great [50]. However, Fig. 12b again shows that even though the magnitudes of the polarisation may change, the ^{h}f value is a constant.

Fouling of the electrodes has long been known to represent a potential source of the variations in the magni-

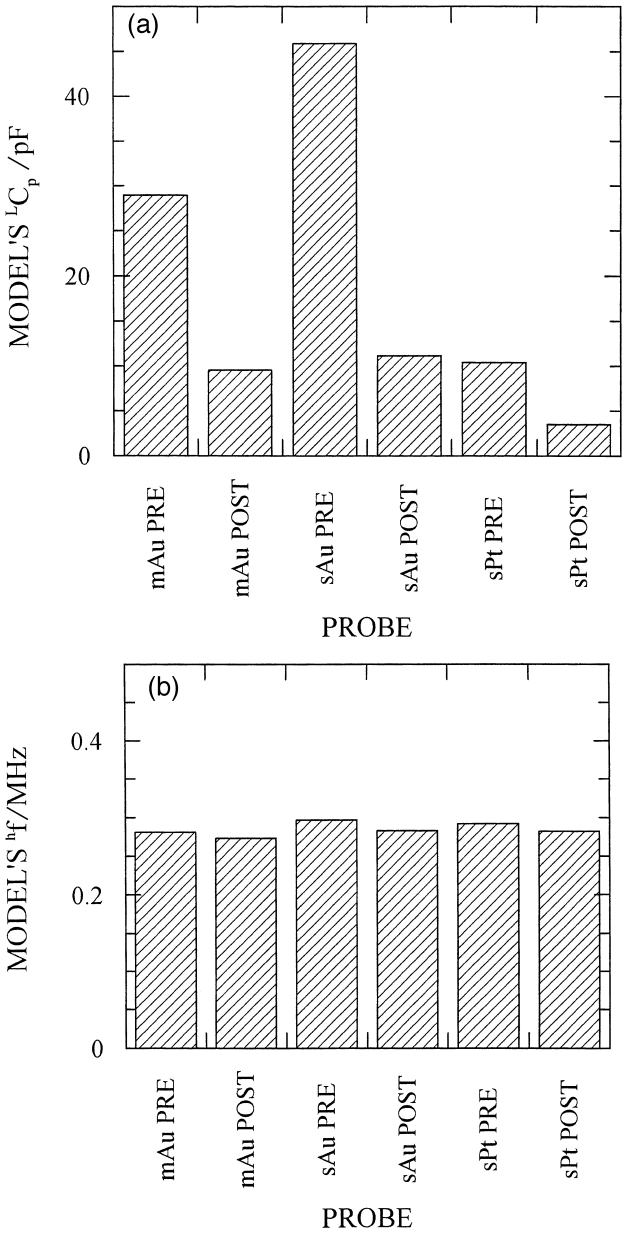

Fig. 14. The effect of applying 10 electrolytic cleaning pulses on the $^{L}C_{p}$ (a) and ^{h}f (b) of the three probes as judged using 120 mM KCl. Each probe was scanned to give the 'pre' data and then cleaned to give the 'post' data. The experiments were done in the order shown from left to right.

tude of electrode polarisation seen during fermentations. To investigate this, the mAu probe was scanned in 120 mM KCl and then in a lysed yeast suspension with the same conductance as that of the KCl solution (see Section 2 for details). Fig. 13a and b shows the ${}^{L}C_{p}$ and ${}^{h}f$ results, which once again shows that the ${}^{h}f$ is maintained at the value seen in all the previous experiments (given a sufficient conductance).

During many fermentations, one is likely to apply the BM's electrolytic cleaning pulses to the electrodes to remove any fouling that may have occurred. To test the effect of this, the three probes were electrolytically cleaned in 120 mM KCl as described in Section 2. Immediately before the cleaning, a control scan in 120 mM KCl was done (pre-pulses scan). The order of the probes in this experiment was randomised. Fig. 14a shows the pre- and post-cleaning pulse ${}^{L}C_{p}$s for each probe. For each of the probes, the cleaning resulted in a drastic reduction in the magnitude of the polarisation, in line with previous observations. The reason for this reduction is probably that the cleaning both removes material adhering to the probes and removes some of the metal, revealing a fresh uncontaminated surface. The problem with using the cleaning pulses to reduce polarisation during fermentations is that after the cleaning, the polarisation can start to increase again and this can make the biomass concentration measured at a spot frequency appear to fall and rise after cleaning is applied. Excessive use of the cleaning can result in metal being put into solution and even routine use of the pulses can result in the probe pins getting a matt finish or being covered in material precipitated out of the fermentation broth. In spite of all of this, Fig. 14b again demonstrates that ${}^{h}f$ is a constant value under these conditions.

The last part of this experiment again involved the mAu probe only. This time, the probe was scanned in 120 mM KCl, then scanned in the lysed yeast, then cleaning pulses applied while in the yeast, and finally rescanned in the yeast. Fig. 15a shows that the decrease in ${}^{L}C_{p}$ caused by the previous set of cleaning cycles was carried over to this part of the experiment. The application of additional cleaning did not reduce the polarisation magnitude any further. Fig. 15b shows that the treatments had little if any effect on the probe's ${}^{h}f$. It thus seems that ${}^{h}f$ is a constant, although of course, different instruments may have different values for this constant.

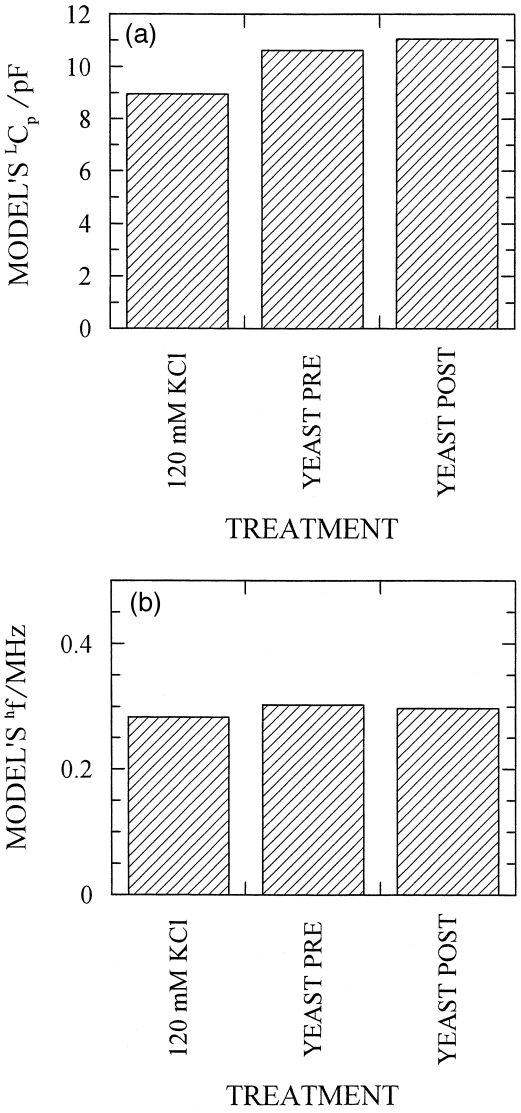

Fig. 15. The effect of applying 10 electrolytic cleaning pulses in the presence of electrode fouling materials on the ${}^{L}C_{p}$ (a) and ${}^{h}f$ (b) of the mAu probe (after the cleaning applied in Fig. 14). The lysed yeast had the same conductance as 120 mM KCl at 1 MHz. The solutions were used in the order shown from left to right with 'pre' referring to the precleaning data and 'post' the data after cleaning.

4. Concluding remarks

We have shown that the electrode polarisation exhibited on a BM follows a power law model and this is in line with work on other electrode types on different machines by different groups. The parameters of this model were modified to give reliable and intuitive measures of the magnitude (${}^{L}C_{p}$) and rate of fall of polarisation with increasing frequency (${}^{h}f$). For the BM, it was shown that although the *magnitude* of electrode polarisation depends strongly on the conductance of the medium and the material of the electrodes, above a certain value of medium conductance (of some 3–7 mS, conductivity = 3.7–8.7 mS cm^{-1}), the value of ${}^{h}f$ is a constant and independent of the conductance of the medium. It is also independent of the electrode metal in the probes, which probe was used, the ionic and other components in the medium, the electrode interface current density, the cell constant, the presence of fouling materials and whether or not any electrolytic cleaning pulses had been applied.

In the following paper [55], we use the results from these experiments to develop a method of reducing the

contribution of electrode polarisation to capacitive biomass measurements and dielectric spectra in general.

Acknowledgements

We thank the BBSRC for financial support and Drs. Hazel Davey, Andrew Woodward and Robert Todd for useful discussions.

Appendix A. Estimating ^{h}f from p

The problem with the linear fit to a log/log plot like Fig. 4 is that the line has the form of Eq. (2) which uses the polarisation capacitance at 1 Hz ($^{1\,Hz}C_p$) as a reference point. To calculate ^{h}f, we need to restate the fitted line in a form that uses ^{L}f as its reference point. The way one does this is to restate the general equation for a straight line in the form given by Eq. (A1.1):

$$y_2 = y_1 + \text{slope}(x_2 - x_1) \quad \text{(A1.1)}$$

The y and x terms refer to the y- and x-axes, respectively. The two points referred to have subscripts 1 and 2 to identify them, with the 2 terms being at the higher x value. By inspection, one can make a log/log plot like Fig. 4 fit this form of a straight line by using ^{L}f and an arbitrary frequency f as the x-axis values, to give upon rearrangement:

$$\log\left(^{f}C_p\right) = \log\left(^{L}C_p\right) + p\log\left(f/^{L}f\right) \quad \text{(A1.2)}$$

By definition, the capacitance due to electrode polarisation at the half frequency is $^{L}C_p/2$. Substituting ^{h}f for f and $^{L}C_p/2$ for $^{f}C_p$ in Eq. (A1.2) gives upon rearrangement:

$$-\log(2) = p\log\left(^{h}f/^{L}f\right) \quad \text{(A1.3)}$$

Anti-logging both sides and then rearranging gives Eq. (3).

References

[1] D.J. Clarke, B.C. Blake-Coleman, R.J.G. Carr, M.R. Calder, T. Atkinson, Monitoring reactor biomass, Trends Biotechnol. 4 (1986) 173–178.
[2] C.L. Davey, H.M. Davey, D.B. Kell, R.W. Todd, An introduction to the dielectric estimation of cellular biomass in real time, with special emphasis on measurements at high volume fractions, Analytical Chimica Acta 279 (1993) 155–161.
[3] C.L. Davey, The Biomass Monitor Source Book, Aber Instruments, Aberystwyth, 1993.
[4] C.L. Davey, The Theory of the β-Dielectric Dispersion and its Use in the Estimation of Cellular Biomass, Aber Instruments, Aberystwyth, 1993.
[5] C.M. Harris, D.B. Kell, The estimation of microbial biomass, Biosensors 1 (1985) 17–84.
[6] D.B. Kell, G.H. Markx, C.L. Davey, R.W. Todd, Real-time monitoring of cellular biomass: methods and applications, Trends in Analytical Chemistry 9 (1990) 190–194.
[7] B.H. Junker, J. Reddy, K. Gbewonyo, R. Greasham, On-line and in-situ monitoring technology for cell density measurement in microbial and animal cell cultures, Bioprocess Eng. 10 (1994) 195–207.
[8] K. Konstantinov, S. Chuppa, E. Sajan, Y. Tsai, S.J. Yoon, F. Golini, Real-time biomass concentration monitoring in animal cell cultures, Trends Biotechnol. 12 (1994) 324–333.
[9] D.B. Kell, B. Sonnleitner, GMP—Good Modelling Practice: an essential component of good manufacturing practice, Trends Biotechnol. 13 (1995) 481–492.
[10] B. Sonnleitner, G. Locher, A. Fiechter, Biomass determination, J. Biotechnol. 25 (1992) 5–22.
[11] G.H. Markx, D.B. Kell, Dielectric spectroscopy as a tool for the measurement of the formation of biofilms and of their removal by electrolytic cleaning pulses and biocides, Biofouling 2 (1990) 211–227.
[12] C.M. Harris, R.W. Todd, S.J. Bungard, R.W. Lovitt, J.G. Morris, D.B. Kell, The dielectric permitivity of microbial suspensions at radio frequencies: a novel method for the real-time estimation of microbial biomass, Enzyme Microbial Technol. 9 (1987) 181–186.
[13] D.B. Kell, C.W. Samworth, R.W. Todd, S.J. Bungard, J.G. Morris, Real-time estimation of microbial biomass during fermentations, using a dielectric probe, Studia Biophysica 119 (1987) 153–156.
[14] D.B. Kell, Forces, fluxes and the control of microbial growth and metabolism. The twelfth Fleming lecture, J. Gen. Microbiol. 133 (1987) 1651–1665.
[15] C.L. Davey, H.M. Davey, D.B. Kell, On the dielectric properties of cell suspensions at high volume fractions, Bioelectrochemistry and Bioenergetics 28 (1992) 319–330.
[16] G.D. Austin, R.W.J. Watson, T.D. Amore, Studies of on-line viable yeast biomass with a capacitance biomass sensor, Biotechnol. Bioeng. 43 (1994) 337–341.
[17] R. Fehrenbach, M. Comberbach, J.O. Pêtre, On-line biomass monitoring by capacitance measurement, J. Biotechnol. 23 (1992) 303–314.
[18] M. Sarra, A.P. Ison, M.D. Lilly, The relationships between biomass concentration, determined by a capacitance-based probe, rheology and morphology of *Saccharopolyspora erythraea* cultures, J. Biotechnol. 51 (1996) 157–165.
[19] I. Cerckel, A. Garcia, V. Degouys, D. Dubois, L. Fabry, A.O.A. Miller, Dielectric spectroscopy of mammalian cells: 1. Evaluation of the biomass of HeLa- and CHO cells in suspension by low-frequency dielectric spectroscopy, Cytotechnology 13 (1993) 185–193.
[20] C.L. Davey, Y. Guan, R.B. Kemp, D.B. Kell, Real-time monitoring of the biomass content of animal cell cultures using dielectric spectroscopy, in: K. Funatsu, et al. (Eds.), Animal Cell Technology Basic and Applied Aspects, Vol. 8, Proceedings of the Japanese Association of Animal Cell Technology, 1997, pp. 61–65.
[21] G.H. Markx, C.L. Davey, D.B. Kell, P. Morris, The dielectric permitivity at radio frequencies and the Bruggeman probe: novel techniques for the on-line determination of biomass concentrations in plant cell cultures, J. Biotechnol. 20 (1991) 279–290.
[22] G.H. Markx, H.J.G. ten Hoopen, J.J. Meijer, K.L. Vinke, Dielectric spectroscopy as a novel and convenient tool for the study of the shear sensitivity of plant cells in suspension culture, Biotechnology 19 (1991) 145–157.
[23] G.J. Salter, D.B. Kell, L.A. Ash, J.M. Adams, A.J. Brown, R. James, Hydrodynamic deposition: a novel method of cell immobilization, Enzyme Microbial Technol. 12 (1990) 419–430.
[24] V. Degouys, I. Cerckel, A. Garcia, J. Harfield, D. Dubois, L. Fabry, A.O.A. Miller, Dielectric spectroscopy of mammalian cells: 2. Simultaneous in situ evaluation by aperture impedance pulse spectroscopy and low-frequency dielectric spectroscopy of the biomass of HTC cells on Cytodex 3, Cytotechnology 13 (1993) 195–202.
[25] C.L. Davey, W. Penaloza, D.B. Kell, J.N. Hedger, Real-time moni-

toring of the accretion of *Rhizopus oligosporus* biomass during the solid-substrate fermentation, World J. Microbiol. Biotechnol. 7 (1991) 248–259.
[26] W. Penaloza, C.L. Davey, J.N. Hedger, D.B. Kell, Stimulation by potassium of the growth of *Rhizopus oligosporus* during liquid- and solid-substrate fermentations, World J. Microbiol. Biotechnol. 7 (1991) 260–268.
[27] W. Penaloza, C.L. Davey, J.N. Hedger, D.B. Kell, Physiological studies on the solid-state Quinoa fermentation, using on-line measurements of fungal biomass production, J. Sci. Food Agric. 59 (1992) 227–235.
[28] N.G. Stoicheva, C.L. Davey, G.H. Markx, D.B. Kell, Dielectric spectroscopy: a rapid method for the determination of solvent biocompatibility during biotransformations, Biocatalysis 2 (1989) 245–255.
[29] G.J. Salter, D.B. Kell, Rapid determination, using dielectric spectroscopy, of the toxicity of organic solvents to intact cells, Fundamentals of Biocatalysis in Non-conventional Media, Elsevier, Amsterdam, 1992, pp. 291–297.
[30] C.L. Davey, G.H. Markx, D.B. Kell, On the dielectric method of monitoring cellular viability, Pure Appl. Chem. 65 (1993) 1921–1926.
[31] G.J. Salter, D.B. Kell, Solvent selection for whole cell biotransformations in organic media, CRC Crit. Rev. Biotechnol. 15 (1995) 139–177.
[32] D.B. Kell, R.W. Todd, Dielectric estimation of microbial biomass using the Aber instruments biomass monitor, Trends Biotechnol. 16 (1998) 149–150.
[33] C.A. Boulton, P.S. Maryan, D. Loveridge, The application of a novel biomass sensor to the control of yeast pitching rate, Proc. Eur. Brewing Convention Congr., Zurich, 1989, pp. 653–661.
[34] R. Pethig, Dielectric and Electronic Properties of Biological Materials, Wiley, Chichester, 1979.
[35] E.H. Grant, R.J. Sheppard, G.P. South, Dielectric Behavior of Biological Molecules in Solution, Clarendon Press, Oxford, 1978.
[36] R. Pethig, D.B. Kell, The passive electrical properties of biological systems: their significance in physiology, biophysics and biotechnology, Phys. Med. Biol. 32 (1987) 933–970.
[37] S. Takashima, Electrical Properties of Biopolymers and Membranes, Adam Hilger, Bristol, 1989.
[38] C.L. Davey, D.B. Kell, The low-frequency dielectric properties of biological cells, Bioelectrochemistry of Cells and Tissues, Birkauser, Zurich, 1995, pp. 159–207.
[39] K.R. Foster, H.P. Schwan, Dielectric properties of cells and tissues: a critical review, CRC Crit. Rev. Biomed. Eng. 17 (1989) 25–102.
[40] D.B. Kell, The principles and potential of electrical admittance spectroscopy: an introduction, Biosensors: Fundamentals and Applications, Oxford Univ. Press, Oxford, 1987, pp. 427–468.
[41] D.B. Kell, C.L. Davey, Conductimetric and impedimetric devices, Biosensors: A Practical Approach, Oxford Univ. Press, Oxford, 1990.
[42] G.H. Markx, C.L. Davey, D.B. Kell, The permitistat: a novel type of turbidostat, J. Gen. Microbiol. 137 (1991) 735–743.
[43] A. Irimajiri, T. Hanai, A. Inouye, Evaluation of a conductometric method to determine the volume fraction of the suspensions of biomembrane-bounded particles, Experientia 31 (1975) 1373–1374.
[44] S.A. Siano, Biomass measurement by inductive permitivity, Biotechnol. Bioeng. 55 (1997) 289–304.
[45] K. Mishima, A. Mimura, Y. Takahara, K. Asami, T. Hanai, On-line monitoring of cell concentrations by dielectric measurements, J. Ferment. Bioeng. 72 (1991) 291–295.
[46] K. Mishima, A. Mimura, Y. Takahara, On-line monitoring of cell concentrations during yeast cultivation by dielectric measurements, J. Ferment. Bioeng. 72 (1991) 296–299.
[47] G.H. Markx, C.L. Davey, D.B. Kell, To what extent is the magnitude of the Cole–Cole α of the β-dielectric dispersion of cell suspensions explicable in terms of the cell size distribution?, Biochem. Bioenerg. 25 (1991) 195–211.
[48] D.B. Kell, Dielectric properties of bacterial chromatophores, Bioelectrochem. Bioenerg. 15 (1983) 405–415.
[49] D.B. Kell, C.M. Harris, Dielectric spectroscopy and membrane organisation, Bioelectricity 4 (1985) 317–348.
[50] C.L. Davey, G.H. Markx, D.B. Kell, Substitution and spreadsheet methods for fitting dielectric spectra of biological systems, Eur. Biophys. J. 18 (1990) 255–265.
[51] H.P. Schwan, Determination of biological impedances, Physical Techniques in Biological Research, Vol. VIB, Academic Press, New York, 1963, pp. 323–407.
[52] H.P. Schwan, Electrode polarization impedance and measurements in biological materials, Ann. NY Acad. Sci. 148 (1968) 191–209.
[53] B. Onaral, H.H. Sun, H.P. Schwan, Electrical properties of bioelectrodes, IEEE Trans. Biomed. Eng. BMI 31 (1984) 827–832.
[54] B. Rigaud, J.P. Morucci, N. Chauveau, Bioelectrical impedance techniques in medicine: 1. Bioimpedance measurement—second section: impedances spectrometry, Crit. Rev. Biomed. Eng. 24 (1996) 257–351.
[55] C.L. Davey, D.B. Kell, The influence of electrode polarisation on dielectric spectra, with special reference to capacitive biomass measurements: (II). Reduction in the contribution of electrode polarisation to dielectric spectra using a two-frequency method, Bioelectrochem. Bioenerg. 46 (1998) 105–114.
[56] A.M. Woodward, A. Jones, Z. Xin-zhu, J. Rowland, D.B. Kell, Rapid and non-invasive quantification of metabolic substrates in biological cell suspensions using non-linear dielectric spectroscopy with multivariate calibration and artificial neural networks. Principles and applications, Bioelectrochem. Bioenerg. 40 (1996) 99–132.
[57] D.B. Kell, C.L. Davey, On fitting dielectric spectra using artificial neural networks, Bioelectrochem. Bioenerg. 28 (1992) 425–434.
[58] D.J. Nicholson, D.B. Kell, C.L. Davey, Deconvolution of the dielectric spectra of microbial cell suspensions using multivariate calibration and artificial neural networks, Bioelectrochem. Bioenerg. 39 (1996) 185–193.
[59] M. Watanabe, T. Suzaki, A. Irimajiri, Dielectric behavior of the frog lens in the 100-Hz to 500-MHz range: simulation with an allocated ellipsoidal shells model, Biophys. J. 59 (1991) 139–149.
[60] H.P. Maruska, J.G. Stevens, Technique for extracting dielectric permittivity from data obscured by electrode polarisation, IEEE Trans. Electrical Insul. 23 (1988) 197–200.